ELSEVIER

Marine Geology 209 (2004) 45–67

MARINE GEOLOGY
INTERNATIONAL JOURNAL OF MARINE GEOLOGY, GEOCHEMISTRY AND GEOPHYSICS

www.elsevier.com/locate/margeo

Holocene development of the Yellow River's subaqueous delta, North Yellow Sea

J. Paul Liu[a,*], John D. Milliman[b], Shu Gao[c], Peng Cheng[d]

[a] *Department of Marine, Earth and Atmospheric Sciences, North Carolina State University, Raleigh, NC 27695, USA*
[b] *School of Marine Science, College of William & Mary, VA 23062, USA*
[c] *Deptartment of Geo-Ocean Science, Nanjing University, Nanjing 210093, China*
[d] *Marine Sciences Research Center, Stony Brook University, NY 11794, USA*

Received 21 October 2002; received in revised form 7 June 2004; accepted 7 June 2004

Abstract

High-resolution seismic profiles from the North Yellow Sea reveal a 20–40-m-thick subaqueous clinoform delta that wraps around the eastern end of the Shandong Peninsula, extending into the South Yellow Sea. This complex sigmoidal-oblique clinoform, containing an estimated 400 km^3 of sediment, overlies prominent relict transgressive surfaces. The nearshore topset of the clinoform, $<$30-m water depth, has a $\ll$1:1000 gradient, with high sedimentation rates (^{210}Pb) $\sim$ 6–12 mm/year. Foreset beds (30–50 m) dip seaward at a steeper gradient (2:1000) and have sedimentation rates $\sim$ 3 mm/year. Bottomset strata, in water depths >50 m, contain less than 1 m of Holocene sediment, with low sedimentation rates, $<$1 mm/year. In contrast to other clinoforms, the Shandong clinoform appears to be a compound subaqueous deltaic system, with what we interpret to be proximal and distal phases of clinoform development. The underlying proximal sequence formed proximally between $\sim$ 11 and 9.2 ka in response to a temporary pause in the rapid postglacial sea-level rise after the meltwater pulse 1B (MWP-1B) and increased discharge from the Yellow River to the North Yellow Sea due to intensification of the summer monsoon. A flooding surface appears to separate the proximal and distal phases, corresponding to the next rapid sea-level rise 9.5–9.2 ka BP (MWP-1C). Since 9.2 ka BP, an overlying distal sedimentary sequence has accumulated, reflecting the back-stepping and shifting river mouth westward to the Gulf of Bohai. Some inputs from coastal erosion and nearby small streams may be locally important. Along-shore transport, cross-shelf advection, and upwelling in the North Yellow Sea have reworked post-LGM sediment and have helped maintain the morphology of the clinoform in the Shandong mud wedge.

Keywords: epicontinental sea; Yellow Sea; Yellow River; subaqueous delta; seismic; clinoform; sea level

1. Introduction

Rivers and their deltas serve as the primary pathway for the transport of fresh water and terrigenous sediment to the coastal ocean (Milliman and Meade, 1983). The morphology of deltas, which constitute an important component within stratigraphic sequences in both modern and ancient continental margins (Morgan, 1970), is largely controlled by the fluvial, tidal, and wave regime (Wright and Coleman, 1973). Equally prominent off many large river mouths are subaqueous clinoforms, meters in height and tens of

* Corresponding author. Tel.: +1-919-515-7977.
E-mail addresses: jpliu@ncsu.edu (J.P. Liu), milliman@vims.edu (J.D. Milliman).

0025-3227/$ - see front matter © 2004 Elsevier B.V. All rights reserved.
doi:10.1016/j.margeo.2004.06.009

kilometers in horizontal extent, characterized by relatively flat topset beds, steeper foresets, and gradual bottom sets. Modern examples include clinoforms off the Amazon (Nittrouer et al., 1986), the Yellow River (Huanghe) (Alexander et al., 1991), the Ganges–Brahmaputra (G–B) (Kuehl et al., 1997), and the Yangtze (Changjiang) (Chen et al., 2000) rivers.

As with other sedimentary features, clinoform development and resultant geometry are dictated by the complex interplay of sediment supply, depositional environment, and the extent and rate of the rise/fall of relative sea level. Kuehl et al. (1986) attributed the low accumulation rates (< 1 mm/year) on the Amazon clinoform topset (< 20-m water depth) to energetic physical conditions. Decreased wave and tidal energy on the thick foreset beds at 30–60-m water depth results in higher rates of sediment accumulation, as great as 100 mm/year. Accumulation in bottomset (>70-m water depth) strata decreases in response to reduced sediment supply. High-resolution seismic profiles on the Bengal shelf also show highest accumulation rates (≥ 50 mm/year) in the foreset region of the G–B subaqueous delta (30–60-m water depth) and lowest (< 3 mm/year) in the bottomset (60–80-m water depth) (Kuehl et al., 1997). A similar stratigraphy has been described for the Yangtze subaqueous delta (Chen et al., 2000).

Many subaqueous clinoforms seem to overlie a transgressive layer 60 m more below present-day sea level. Beyond seaward limit of the Yangtze subaqueous bottomset, at 60–70 m, for example, sediments are composed of grayish yellow, well-sorted fine to medium–fine sands containing shallow-water shells (Chen et al., 2000), representing relict sediments deposited during the last regression, low-stand and subsequent transgression of sea level (Saito et al., 1998). Thus, understanding of the geometry and formation of subaqueous clinoforms requires not only a knowledge of present-day environmental conditions, but also of sea-level history.

The modern Yellow River, which presently discharges into the western Bohai Sea (Fig. 1), is widely recognized as having (together with the Amazon and Ganges–Brahmaputra) the highest sediment load on

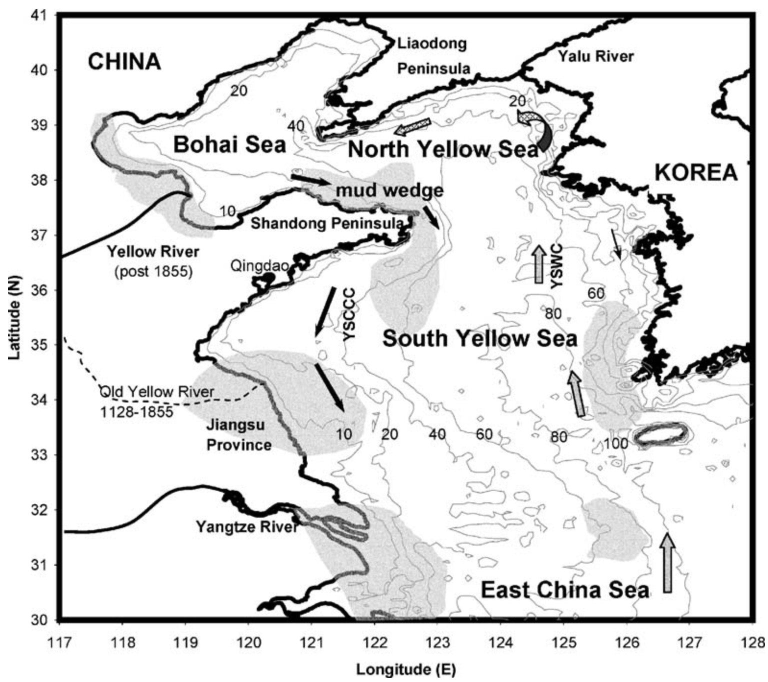

Fig. 1. Location and bathymetric map of the Bohai Sea (BS), North Yellow Sea (NYS), South Yellow Sea (SYS), and East China Sea (ECS). The Yellow Sea Warm Current (YSWC) and the Yellow Sea Coastal Cold Current (YSCCC). Shaded areas represent location of the Shandong mud wedge and other mud patches in the YS and ECS. Water depth in meters.

Earth, about 10^9 t/year (Qian and Dai, 1980; Milliman and Syvitski, 1992). Highly turbid gravity flows transport some sediment off the modern delta (Wright et al., 1988, 1990), but most of the fluvially derived sediment (>90%) appears to remain trapped within the modern deltaic system (Bornhold et al., 1986, Martin et al., 1993, Wright et al., 2001). In the 1980s, a prominent mud wedge was noted extending southward from the eastern tip of the Shandong Peninsula (Milliman et al., 1987), some 350 km east of the present-day river mouth. Alexander et al. (1991) suggested that this Shandong Subaqueous Delta represents a direct escape route of Yellow River sediment into the South Yellow Sea. More recent work has shown that this clinoform also extends along the northern side of the Shandong Peninsula in the North Yellow Sea (Liu et al., 2002) (Fig. 1). In contrast to Alexander et al. (1991), however, Liu et al. (2002) have suggested that much of this thick mud wedge was probably formed proximally to the paleo-Yellow River mouth in the early Holocene. In this paper, we discuss the high-resolution seismic structure and sedimentary facies in the North Yellow Sea as well as other sedimentological and oceanographic data, which collectively allow us to synthesize the history of this prominent clinoform.

2. Study area

2.1. Bathymetry

The Yellow Sea is a shallow, relatively flat, semi-closed epicontinental sea bordered by China and the Korean peninsula. To the northwest is the very shallow Bohai Sea, with water depths generally less than 40 m. To the south is the East China Sea (Fig. 1), which borders the Okinawa Trough to the south. A NW–SE trough, defined by the 80-m isobath (Fig. 1), transects the eastern part of the Yellow Sea; elsewhere, water depths are shallower. The Shandong Peninsula separates the South from the North Yellow Sea (NYS).

The NYS, the subject of this paper, is defined largely by the 40- and 60-m isobaths. Most of the central portion of the basin is deeper than 50 m and characterized by a relatively flat bottom (Figs. 2 and 3), although large symmetrical bed forms occur in the northeast adjacent to the Yalu River. The apparent symmetrical configuration of these sand ridges suggests that they are heavily influenced by tidal oscillations within the NYS (Qin et al., 1989). Greatest depths in the NYS occur between the Shandong Peninsula and Korea, where depths locally exceed 70 m (Qin et al., 1989).

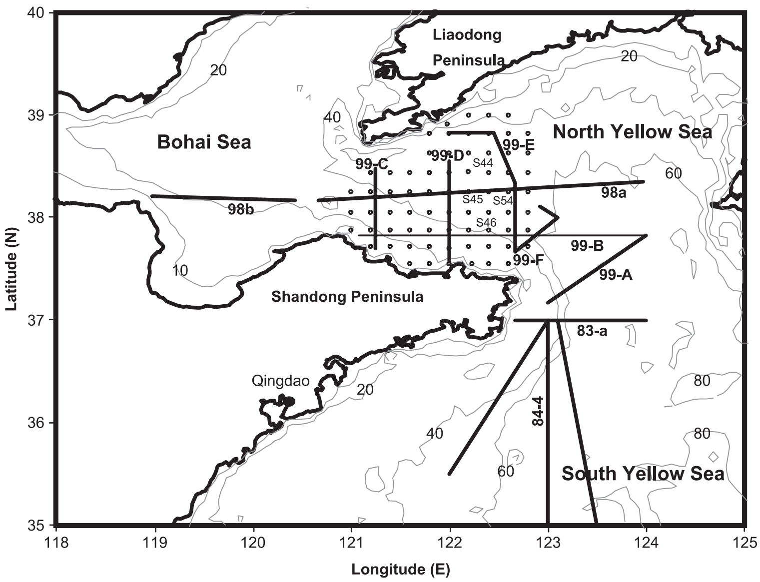

Fig. 2. Seismic profile lines (|) and surface-sediment sample locations (●) in the North Yellow Sea.

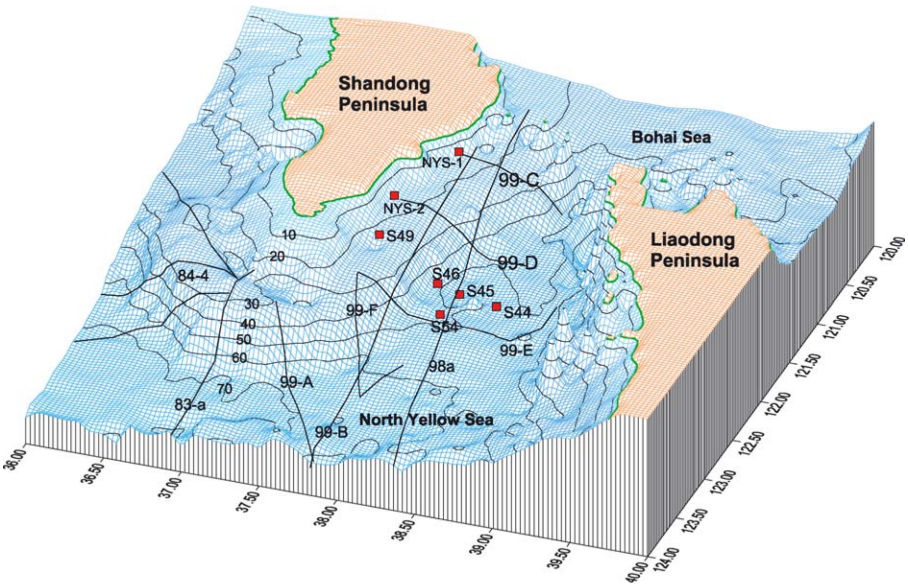

Fig. 3. Three-dimensional seafloor morphology of the North Yellow Sea shows a series of subtle terraces around Shandong Peninsula. It also shows the location of our seismic profiles (black lines) and box and gravity cores (red square boxes) in relation to the clinoform.

The three-dimensional bathymetric morphology (Fig. 3) shows a prominent terrace that wraps around the eastern Shandong Peninsula; we call this feature the Shandong clinoform. Gradients in water depths shallower than about 20–25 m are ≪1:1000, whereas on the clinoform's foresets gradients are 2:1000.

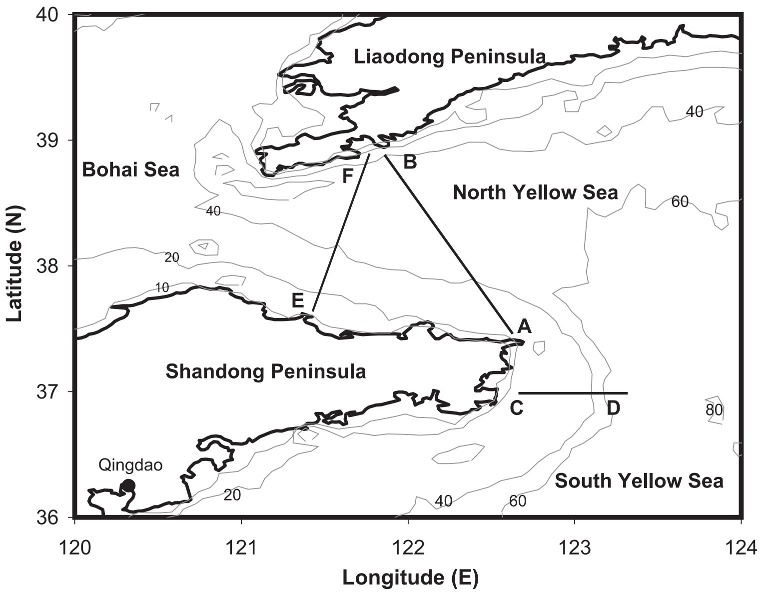

Fig. 4. Transect surveys between C–D (eastern tip of Shandong Peninsula) (Xia and Guo, 1983; Li and Ding, 1996), A–B (cross the NYS from Shandong to Liaodong Peninsula) (Martin et al., 1993; Zhao, 1996), and E–F (across the Bohai strait from Shandong to Liaodong Peninsula) (Martin et al., 1993).

There are, however, several subtle breaks in clinoform topography (Fig. 3). A 5–10-m linear depression is seen in water depths shallower than about 25–40 m (see Profile 99-E in Fig. 10), landward of which the bottom shoals towards the peninsula. As will be discussed later, we suspect that this shallow trough may reflect erosion and eastward transport of clinoform sediment. The other morphologic break occurs at about 45 m in profiles 99-E and 99-F (Fig. 10) and represents what we term the toe of the clinoform (see below).

2.2. Regional oceanography

The general circulation in the North Yellow Sea is characterized by a counterclockwise gyre, with northwestward inflow of Yellow Sea Warm Current (YSWC) in the winter along the eastern and northern sides of the basin and the Yellow Sea Cold Coastal Current (YSCCC) flowing eastward from the Gulf of Bohai along the Shandong Peninsula into South Yellow Sea (Fig. 1). During the winter, strong northwesterly winds drive surface and nearshore transport southward, necessitating a northward return flow at depth. The YSWC, reaching at most about 5 cm/s (Yuan and Su, 1984), produces a warm tongue of water that follows a path along the deepest axis in the eastern SYS and northern NYS basins (Zheng and Klemas, 1982). The YSWC also penetrates into Bohai Sea and plays an important role in forming sand ridges in the east Bohai Sea and dispersing the fine sediments into the west side of the Gulf (Liu et al., 1998).

Temperature and salinity profiles (A–B) across the NYS (Figs. 4–6) based on published hydrographic data indicate that the entire NYS can be well mixed under the influence of strong northwesterly wintertime winds, November (Fig. 5a) and February (Fig. 5b). At

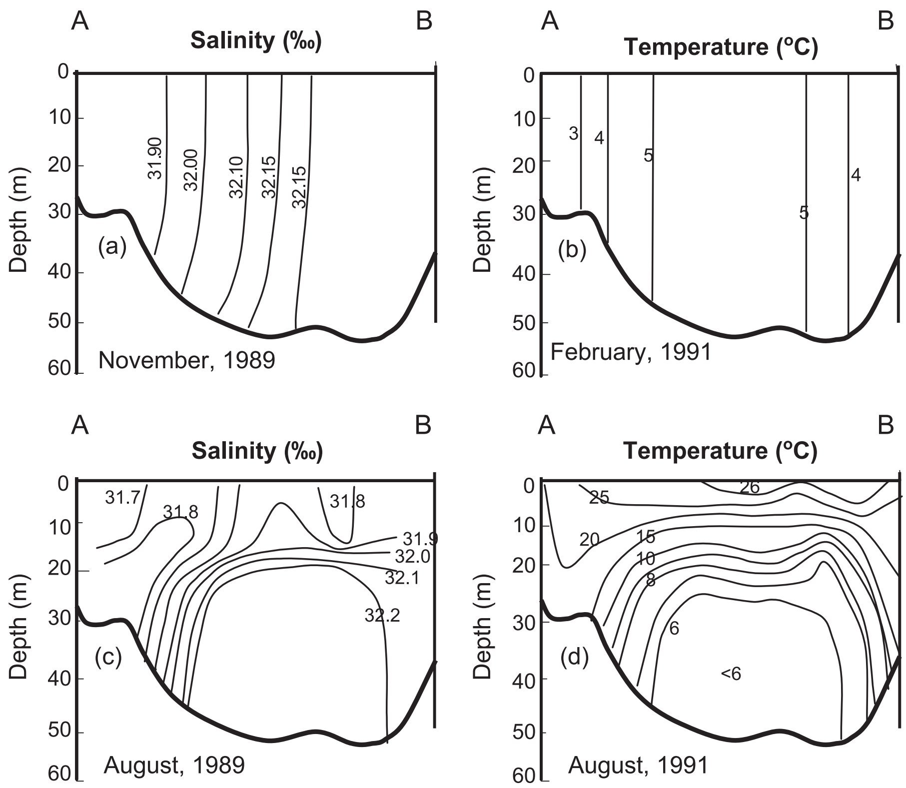

Fig. 5. Vertical profiles of temperature and salinity (1989–1991) of the transect A–B (Fig. 4), which cross the whole NYS, reveal the well-mixed winter conditions (a, b), and stratified summer conditions (c, d) with a cold and saltier water in the central bottom (Martin et al., 1993).

same time, a cold, fresh surface water flows eastward out of the Bohai Sea into the NYS and SYS along the north coast of Shandong Peninsula, and a relative warmer, more saline subsurface counter-current flows westward (Guan, 2000). Suspended sediment concentrations in the wintertime are highest in nearshore regions (cross-section C–D), with values exceeding 50 mg/l (Fig. 6a).

The summertime hydrography across the NYS (A–B) is characterized by a pronounced cold-pool in the deeper basin overlain by 20–25 m of highly stratified warmer water (Figs. 5c and d) (Martin et al., 1993). Stratification breaks down along the boundaries of the NYS, reflecting in part counterclockwise circulation in the NYS and landward upwelling (Zhao, 1996). A sustained cold surface water around eastern tip of the Shandong Peninsula also suggests possible upwelling (Xia and Guo, 1983). More stratified summertime conditions and calmer weather result in the much lower suspended matter concentrations in NYS coastal waters (i.e., C–D and E–F profiles), generally 5–10 mg/l (Fig. 6b and d) (Li and Ding, 1996; Martin et al., 1993). Recent (1995–1997) NOAA-AVHRR satellite images show that high suspended matter concentration in the coastal water of YS and ECS move offshore from November to March, whereas from May to September transport is onshore (Sun et al., 2000). 3-D sediment transport models of the Bohai Sea (Jiang et al., 2000) and Yellow Sea (Yanagi and Inoue, 1995) indicate that although there is indeed some eastward and southward transport of sediment in the winter and early spring, most modern Yellow River-derived sediment remains in the Bohai Sea.

2.3. The Yellow River

The most unique feature of the Yellow Sea is the presence of the Yellow River, which currently discharges into the Gulf of Bohai, but as recently as 1855 discharged south of the Shandong Peninsula along the Jiangsu coast (Fig. 1). Draining arid northern China, the river's discharge historically has been low; its

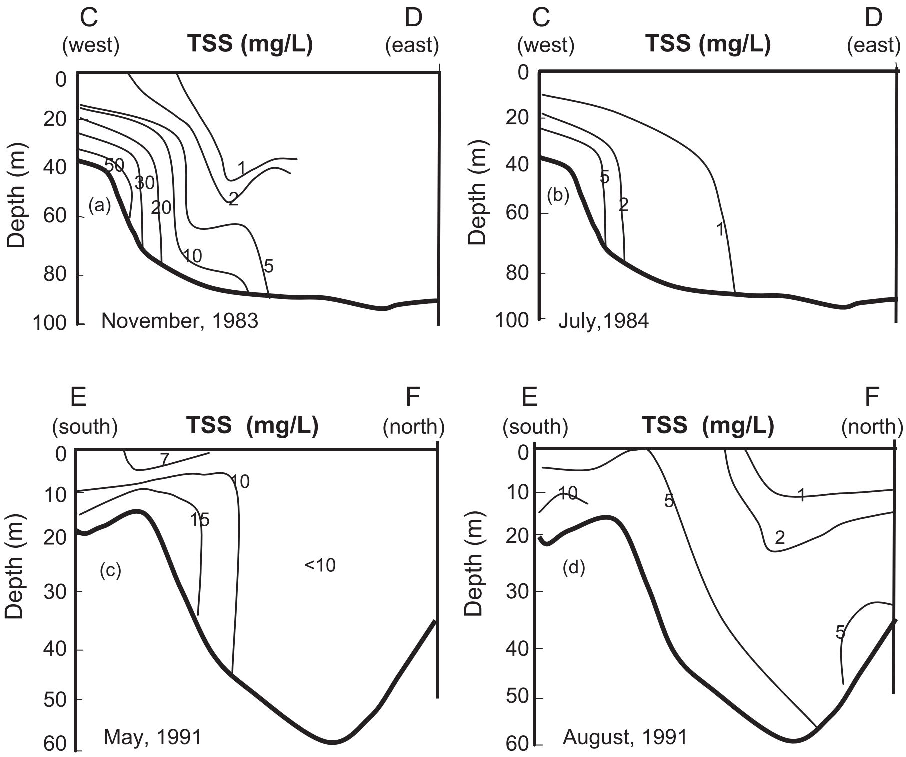

Fig. 6. Vertical profiles of TSS distribution along the transect C–D (Li and Ding, 1996) and E–F (Martin et al., 1993) reveal the higher TSS nearshore bottom in winter (a) and lower value in Summer (b–d). Transect shown in Fig. 4.

large sediment loads come from the easily erodable late Pleistocene loess along the middle reaches of the river, as well as impacts of historically poor farming techniques. Over the past 2000 years or so, the river has discharged about 10^9 t/year of sediment, before which its load may have been as much as an order of magnitude lower (Milliman et al., 1987; Saito and Yang, 1995, Saito et al., 2001). Recently, the river's annual load has dropped considerably in response to improved land conservation, dam construction, and increased water withdrawal due to decreased rainfall (Yang et al., 1998; Galler, 1999).

Because of its historically large sediment load, the Yellow River has meandered frequently, and as a result its course has changed both regionally and locally. In the past 9000 years, there have been 11 documented shifts in the Yellow River's path, at least twice when the river flowed south of the Shandong Peninsula (Saito et al., 2001). Although the first such episode is poorly documented, the river apparently shifted to the south in response to heavy floods ~ 9 ka (Yang et al., 2000) and continued to discharge at the Jiangsu coast for the next 2 ky (Liu et al., 2002). For nearly 6-ky beginning about 7 ka, the river discharged mostly or entirely into the Bohai Sea, before shifting southward again in 1128 AD. The river then again shifted to the north in 1855, where it has prograded the present Yellow River delta nearly 50 km (Saito et al., 2001).

Since sea level reached (or exceeded) its present-day position about 7.5 ka, sediment has accumulated in coastal areas along the Jiangsu coast and on present-day Yellow River delta in the western Bohai. Before that, during the post-LGM sea-level transgression (11–7.5 ka), it accumulated in the SYS and NYS, in response to varying rates of sea-level rise (Liu, 2001) and reinitiation of the SW Monsoon, 11 ka. During this 3.5-ky period, a prominent subaqueous delta formed off the Jiangsu coast in the SYS, presumably the result of the first south-shift of the Yellow River in the early Holocene (9.0–7.0 ka) (Liu et al., 2002). We submit and attempt to prove in this paper that the Shandong mud wedge, abutting the eastern and northern edges of the Shandong Peninsula, is also a relict feature of the Yellow River, formed in response to increased sediment discharge from a strengthened SW (summer) monsoon and a relative still-stand during post-LGM sea-level transgression.

3. Methods

Since the early 1980s, many oceanographic and geological/geophysical cruises have documented the oceanography, morphology, surface sediments, and shallow stratigraphy of the Yellow Sea. Seismic profiles obtained in 1983–1989 as part of a cooperative study between the Institute of Oceanology, Chinese Academy of Sciences (IOCAS), and the Woods Hole Oceanographic Institution (WHOI) helped define the configuration and boundaries of the Shandong clinoform in the South Yellow Sea (Figs. 1 and 2) (Milliman et al., 1989). The distribution and configuration of the clinoform in the Bohai and North Yellow seas described in this paper were defined by geophysical and geological data obtained during two cruises in 1998 and 1999 aboard the RV *Gold Star II* of IOCAS. During these two cruises, we collected approximately 1200 km of high-resolution seismic profiles, 10 gravity cores (four are cited in this study), 70 surface sediment samples (Fig. 2), and 7 box cores (Fig. 3). All seismic data were obtained with a 450-kJ ORE GeoPulse boomer system fired at 0.5-s intervals; records were filtered between 500 and 3000 Hz.

Well-documented peat deposits that underlie the mud wedge in the North Yellow Sea were sampled in the gravity cores (NYS-5) (Fig. 10) and AMS-dated at WHOI's NOSAMS lab. Radiocarbon ages were calculated using 5568 years as the half-life of radiocarbon and are reported in calendar years using the newly updated CALIB4.3 (Stuiver et al., 1998).

^{210}Pb activities were determined from sediments sampled at 2-cm intervals from seven box cores (Fig. 3) to determine short-term rates of sediment accumulation. Sediments were dried, ground, homogenized, and packed in 50-mm diameter petri dishes. After waiting at least 20 days for secular equilibrium of ^{226}Ra daughter isotopes, the samples were counted for 1–3 days by gamma spectrometry, planar germanium detector coupled to a multichannel analyzer. Activities were corrected for shelf-absorption using a radioisotope source (Cutshall et al., 1983). Excess ^{210}Pb activities were calculated by subtracting the supported levels obtained from parent ^{226}Ra activities.

Grain size of the surface sediments was measured after first wet-sieving the samples through a 63-μm sieve. Sand fractions retained on the sieve were dried and sieved. Mud fractions passing through the sieve were pretreated using a dispersing agent (sodium hexametaphosphate) to inhibit flocculation, and then dispersed and homogenized using ultrasound before passing through the Cilas Laser Particle Size Analyzer (model: 940L). Size parameters were calculated based on the methods of McManus (1988).

Oceanographic data (temperature, salinity, current, and total suspended particulate matter) are from historical observations conducted in the NYS between 1959 and 1993 (Xia and Guo, 1983; Milliman et al., 1986; Martin et al., 1993; Li and Ding, 1996; Zhao, 1996) (Fig. 4).

4. Results

4.1. Shallow structure

GeoPulse profiles (Figs. 7–13) show a prominent clinoform, 15–40 m in thickness, that thins offshore to less than 1 m. It abuts the northern slope of the Shandong Peninsula, and wraps around the eastern end of the Peninsula, connecting with the Shandong subaqueous delta (Alexander et al., 1991) that extends into the South Yellow Sea. The clinoform is underlain by a highly reflective surface that locally is acoustically opaque (Figs 7, 9–11, 13) and that lies at or near the seafloor in the central parts of the NYS. Core NYS-5 (Fig. 10) penetrated a dark peat at 120 cm, which AMS ^{14}C dating (calibrated age: 11.8 ky BP) suggests was deposited presumably subaerially when post-LGM sea-level had not yet transgressed into the NYS.

A compact yellow layer, which we interpret to be loess, was recovered at 230 cm in Core S45 (Figs. 12 and 15). We assume that this loess is synchronous with loess exposed along the present-day northern coast of the Shandong Peninsula, and was deposited by the intensified winter monsoon during LGM (Liu and Zhao, 1995). Other cores penetrated stiff clay or silty-sand layers that we assume were deposited subaerially during or before the post-LGM transgression (Kim et al., 1999, Park et al., 1998). Where

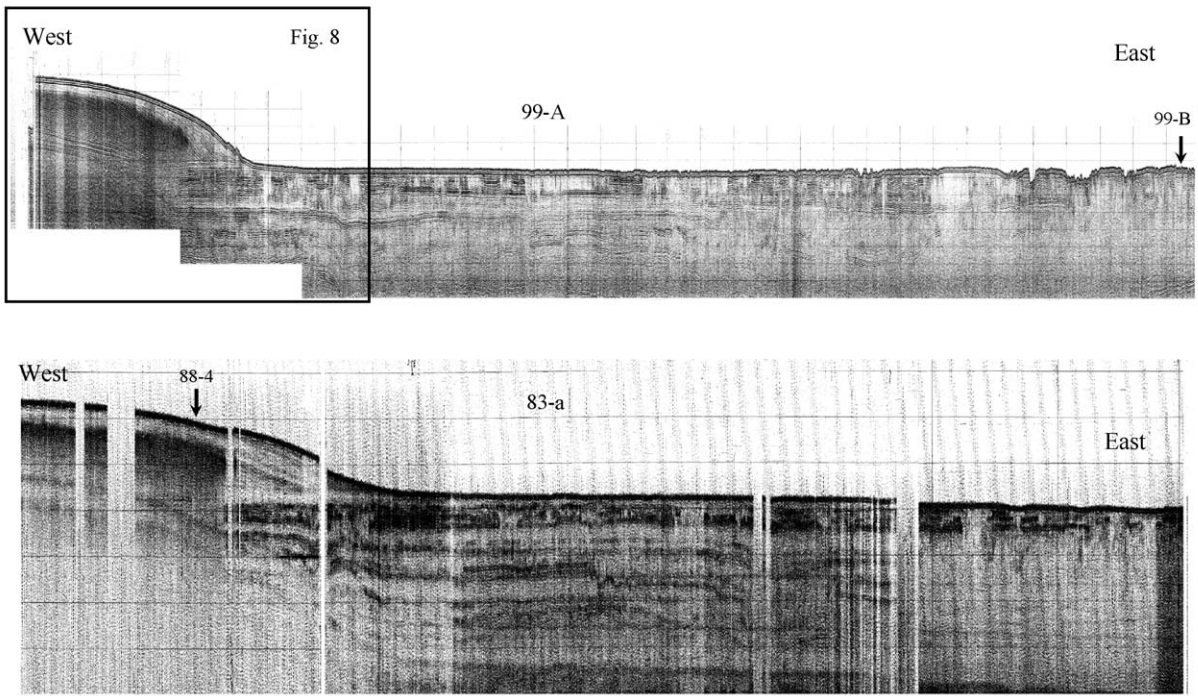

Fig. 7. GeoPulse records from profiles 99-A and 83-a in the east tip of the Shandong Peninsula showing clinoform in the west, and transgressive, ravinement surface in the east. Profile locations are shown in Figs. 2 and 3.

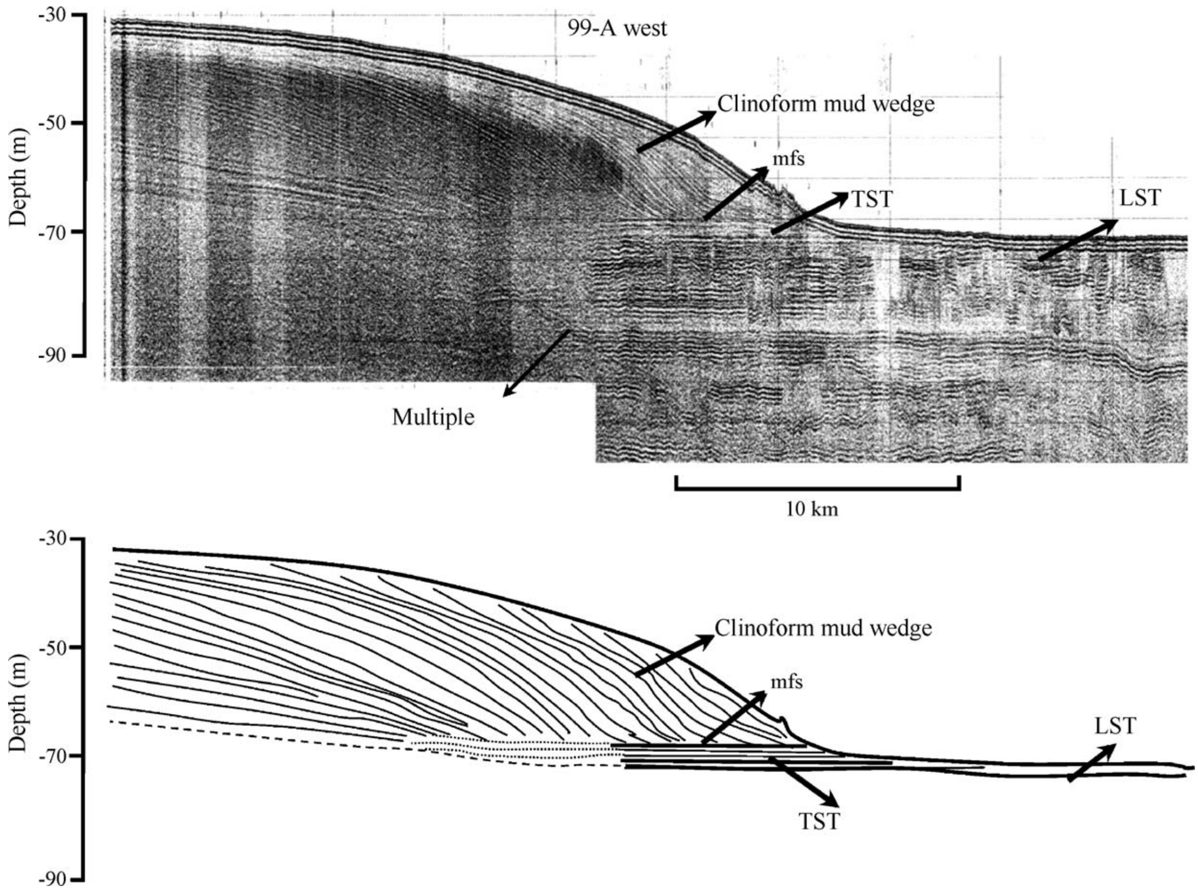

Fig. 8. High-resolution GeoPulse records of the westernmost part of the seismic profile 99-A, show a clinoform structure with the oblique features in the west. The transgressive system tract (TST) culminating with a maximum flooding surface (msf) is seen underlying the later mud deposits. The early-phase bottomset can be seen to be buried by the later foreset deposits. Location of profile is shown in Figs. 2 and 3.

modern muds have been winnowed by strong erosion (e.g., northern end of profile 99-C, near the deep channel in the Bohai Strait; Figs. 11 and 12), these stiff clays lie sufficiently near the seafloor to be sampled with a grab. We therefore conclude that this acoustically reflective surface represents a combination of low-stand stiff silts and clays, and post-LGM peaty deposits.

Locally, subparallel semitransparent layers are seen to lie beneath the acoustic reflective surface (Figs. 8–10), truncated by a prominent erosional surface (profile 99-B in Fig. 9). Some profiles show this layer to be filled with acoustically reflective strata, suggesting a transgressive systems tract (TST) (Figs. 8–10), while to the east this surface appears to outcrop at the seafloor (Fig. 7). Perhaps the best evidence of the nature and age of transgressive surface is seen in Profile 99-C, where strong currents near the Bohai Strait have removed the acoustically opaque post-LGM strata, exposing the morphologically uneven ravinement surface (Fig. 11, top). Close inspection of the seismic profiles (e.g., 99-E, Fig. 10; 83-a; Fig. 7) shows several deeper reflective surfaces, which we assume represent position of the former sea level before last transgression.

In the NYS, the clinoform is thickest in the east and thins to less than 15 m in the west (Profile 99-C; Fig. 11); it apparently is poorly defined or nonexistent in the Bohai Sea (Fig. 12). The shape of this clinoform in the west (such as 99-C) shows a typical sigmoidal structure, but most of others show oblique to complex sigmoidal–oblique clinoform. Topset gradients are

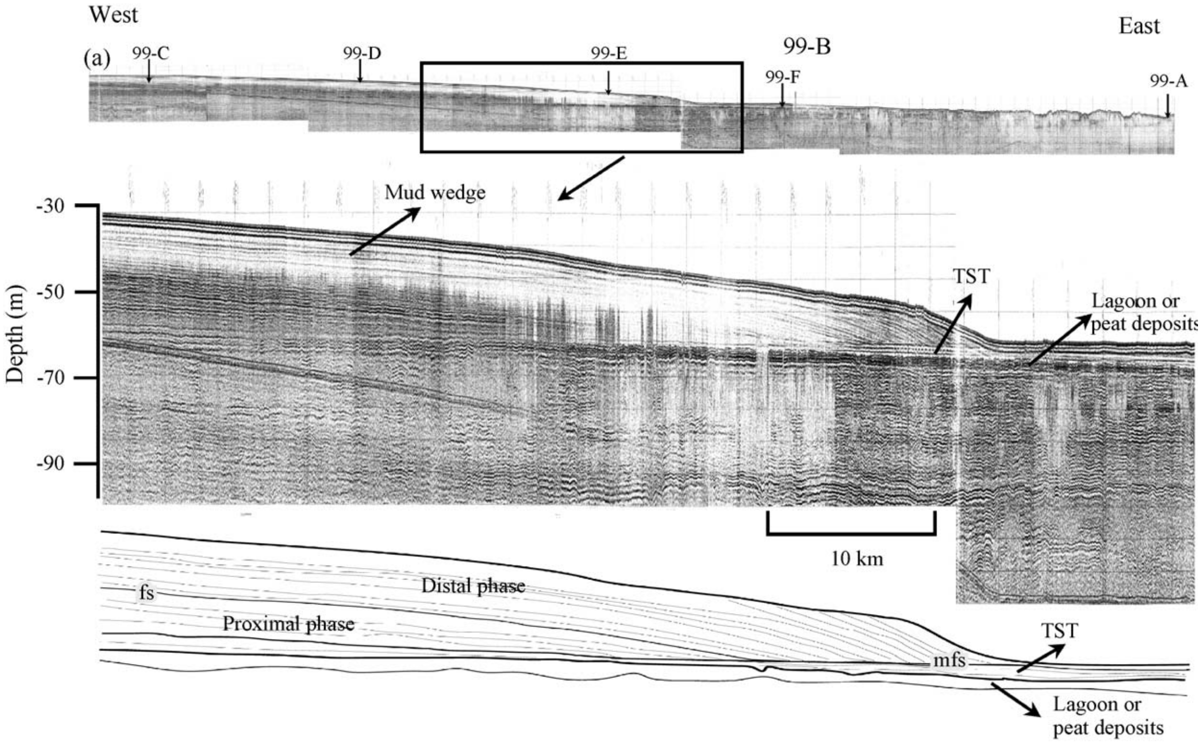

Fig. 9. GeoPulse record of profile 99-B from the eastern NYS the western NYS in along the shoreshore of north Shandong Peninsula, which shows the seaward and eastward progradation of the mud wedge. An enlargement of the clinoform's toe and easternmost part is shown below. Location of profile is shown in Figs. 2 and 3.

much less than 1/1000, whereas foreset gradients are about 2/1000 (Fig. 3). Sediment volume within the entire Shandong clinoform is roughly estimated to be about 300 km^3, of which about 200 km^3 are in the NYS (Liu et al., 2002).

Careful inspection of many of the clinoform profiles shows a rather complex inner structure, perhaps best seen in Profiles 99-A, B, and F (Figs. 8–10). The lower part of the clinoform lying under the topset and foreset beds tends to be acoustically "turbid", and in Profile 99-F this turbid layer conforms with a reflector that lies about 7–8 m beneath the upper part of the foreset and ~ 15 m beneath the lower foreset. The turbid layer is seen on all other profiles except Profile 99-C, in the far west of the NYS. Judging from other clinoforms (Nittrouer et al., 1996; Diaz et al., 1996), this turbid layer presumably indicates the presence of biogenic gas. Strata overlying the turbid layer, in contrast, are acoustically transparent, locally to the extent that individual reflectors are difficult to delineate. A closer inspection of the profiles indicates that the "toe" described above consists of younger prograding strata (Figs. 9 and 10). Existence of the biogenic gas and the distinct acoustic reflections/features implicate different sediment composition and depositional processes. The gas-discharged layer in the lower part of the clinoform is apparently mainly composed of silts to silt-sands, in contrast with the clay-silt dominated upper layer (Fig. 15). The significance of this is discussed below.

4.2. Sediments and recent rates of sediment accumulation (^{210}Pb)

Surface sediments throughout the NYS are characterized by medium to fine silts, with the finest sediment occurring near the Shandong Peninsula and in the central part of the basin (Fig. 14); sand generally constitutes less than 5–10% of the sediments. Interrupting this pattern, however, are two tongues of

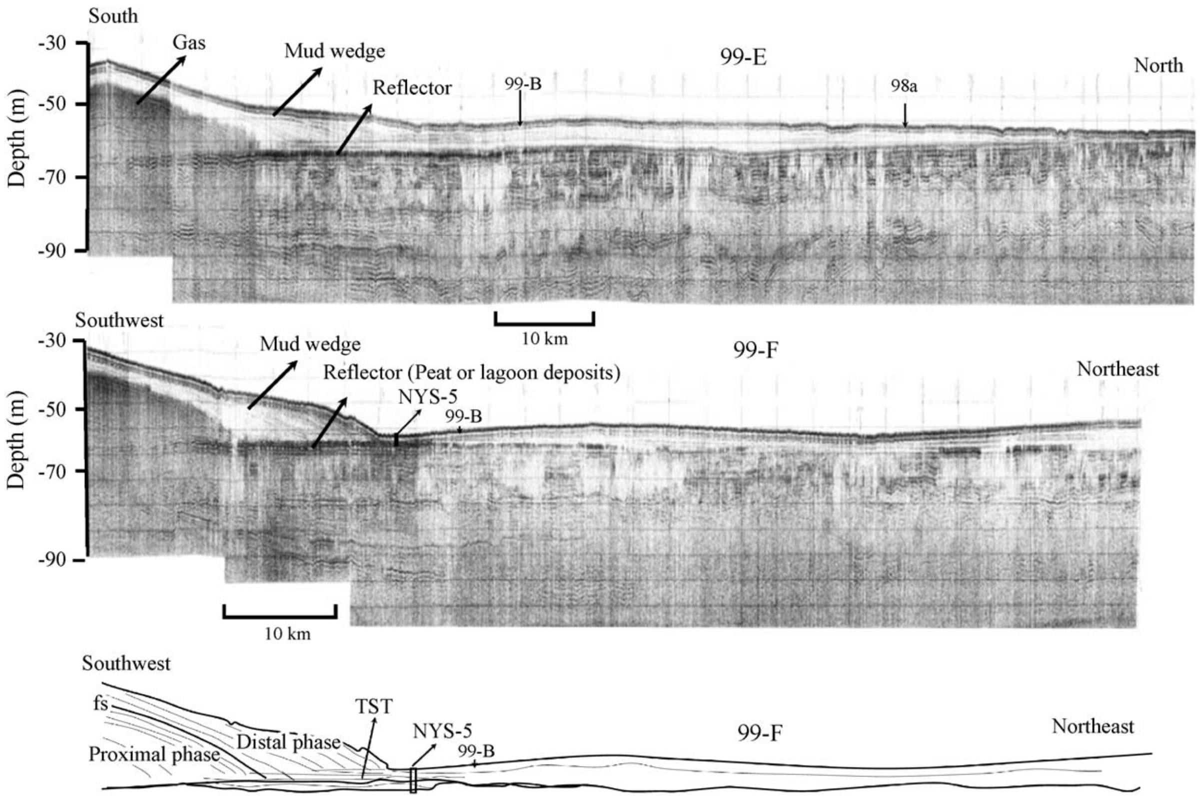

Fig. 10. GeoPulse profiles 99-E and 99-F. The gravity core of NYS-5 recovered a peat sample that apparently underlies the soft and transparent mud deposits; this peat layer might represent the strong reflective surface seen in these profiles. Biogenic methane gas is evident in the record on the landward, and limits penetration of the acoustic signal. Location of profiles is shown in Figs. 2 and 3.

coarser sediment, one along the northeastern NYS and the other along the southwestern NYS (Cheng and Gao, 2000). In the northern NYS, the coarse silty-sand surface is consistent with the transgressive surface recorded in the seismic profiles (see below).

Four gravity cores taken on the NYS clinoform (S44 and S54 on the bottomset; S45 close to the foreset; and S46 in the foreset; Fig. 3) show the general dominance of clay- and silt-size components (Fig. 15). Sand is essentially completely absent from both the foreset core S46 and bottomset core S54, and only few shell fragments are present in the bottom of S54. In contrast, sand is a prominent constituent below about 40 cm in bottomset core S44, reaching >20% in some layers, and shell fragments are prominent at the bottom of the core. Sand also is present below 180 cm in bottomset core S45, and below 230 cm there is a yellowish, stiff sandy-silt, suggesting a relict loess, separated from the overlain layer by an unconformity (Fig. 15). The internal differences of the sediment character may not only reflect the different depositional environment, but also provide the explanation of the existence of the subsurface gas, which was released from the underlying peat, formed before the transgression at ~ 14–12 ka BP.

Sedimentation rates based on ^{210}Pb geochronology from the seven box cores show a differentiation from the topset (NYS-1, NYS-2, S49), foreset (S45, S46), and bottomset (S44, S54) strata Figs. 3, 16 and 17). The two topset cores (NYS-1 and NYS-2), along the Shandong Peninsula (Fig. 3), display maximum accumulation rates of 12.4 and 6.4 mm/year (Fig. 17). The scatter plot (Fig. 17) from the topset core (S49) may indicate either extensive biogenic reworking or physical mixing. In contrast, the two foreset cores (S45, S46) display relatively high accumulation rates of 2.9

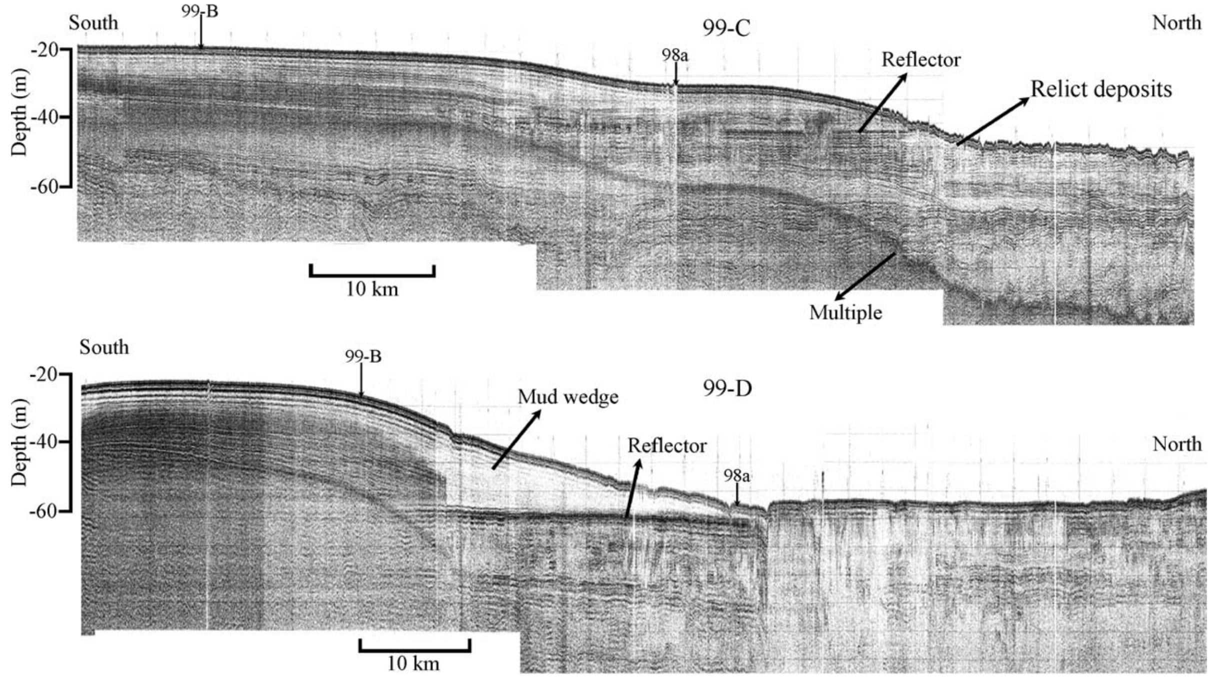

Fig. 11. GeoPulse record of profile of 99-C in the west NYS and 99-D across the central NYS from south to north. 99-C does not display the transparent character seen in other profiles, which indicate a coarser size fraction. Location of profiles is shown in Figs. 2 and 3.

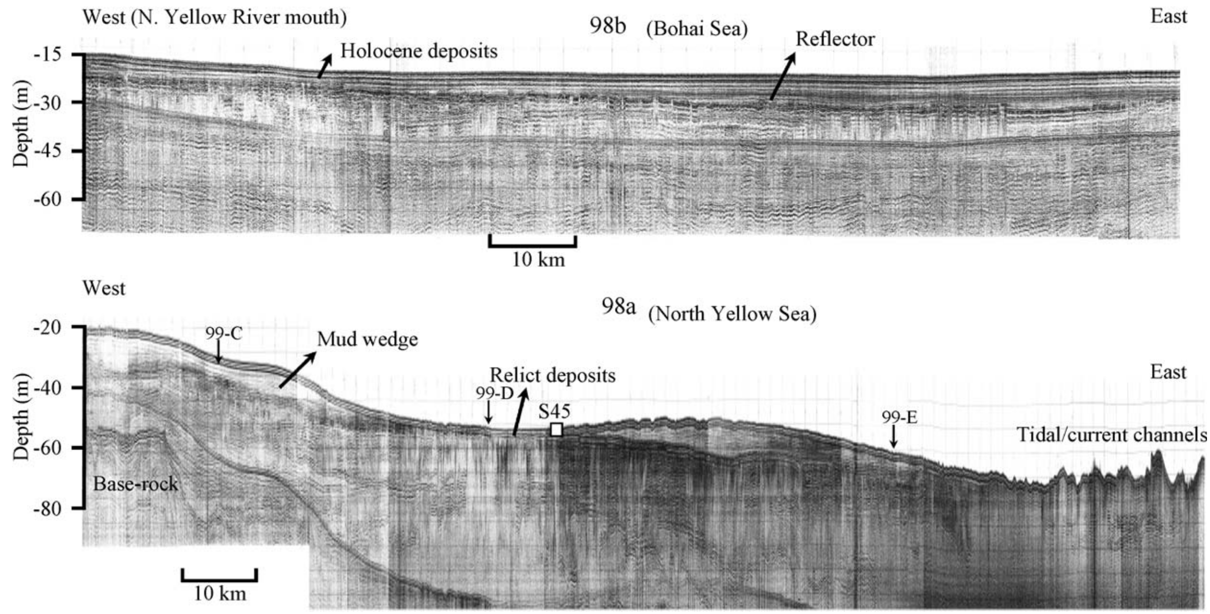

Fig. 12. Gravity core of S45 reveals the apparent eolian loess deposits lying beneath ''modern'' muds (also see Fig. 15). This loess may reflect the lowstand LGM depositional environment. Profile 98b indicates less than 10-m Holocene sediments in the eastern part of the NYS and the Bohai Sea. Location of core is shown in Fig. 2.

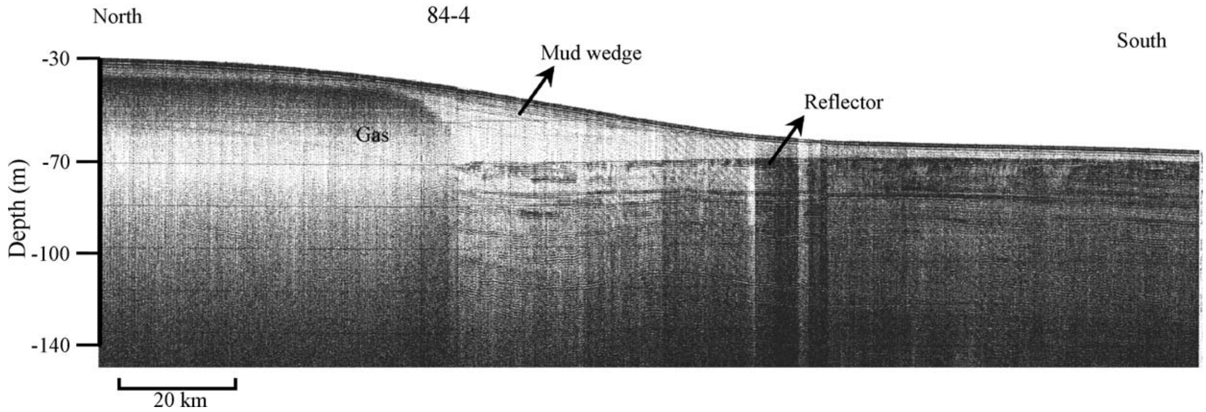

Fig. 13. GeoPulse profile 84-4, extending southward from the tip of Shandong Peninsula into the central South Yellow Sea, reveals the gas-charged southward-trending clinoform. Location of profile is shown in Figs. 2 and 3.

and 3.9 mm/year, respectively (Fig. 16). Accumulation rates in the bottomset strata are significantly less, 0.7 and 0.9 mm/year for S44 and S54, respectively (Fig. 16).

5. Development of the Shandong clinoform

Being nowhere deeper than about 70 m, the semi-enclosed North Yellow Sea was entirely subaerially

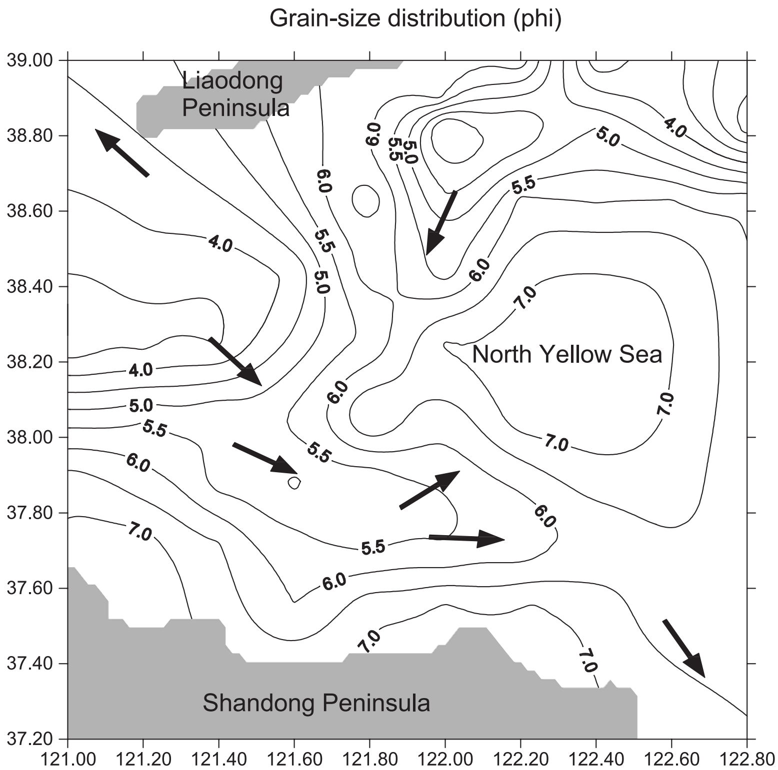

Fig. 14. Distribution of grain size in the surface samples. Net sediment transport patterns can be obtained based on grain size trend analysis (after Cheng and Gao, 2000). Sample locations are shown in Fig. 2.

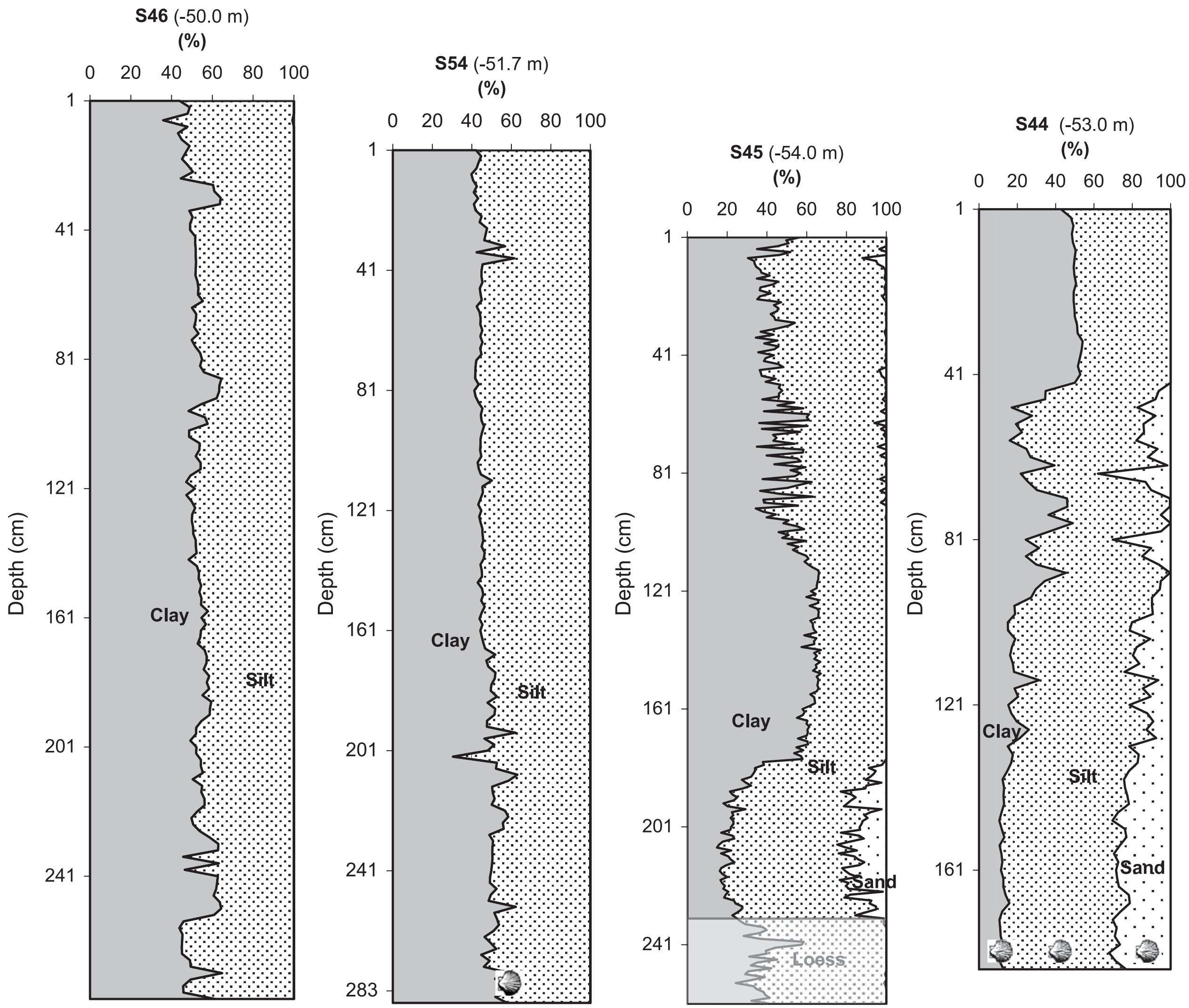

Fig. 15. Stratigraphic transect through the foreset to bottomset. Thin mud (clayey-silt) was found in the offshore of central NYS; the thick mud is nearshore. The bottom of S44 and S45 shows a sandy-silt layer that represents the pretransgressive or transgressive deposits that forms the acoustical unconformity. Core locations are shown in Fig. 2.

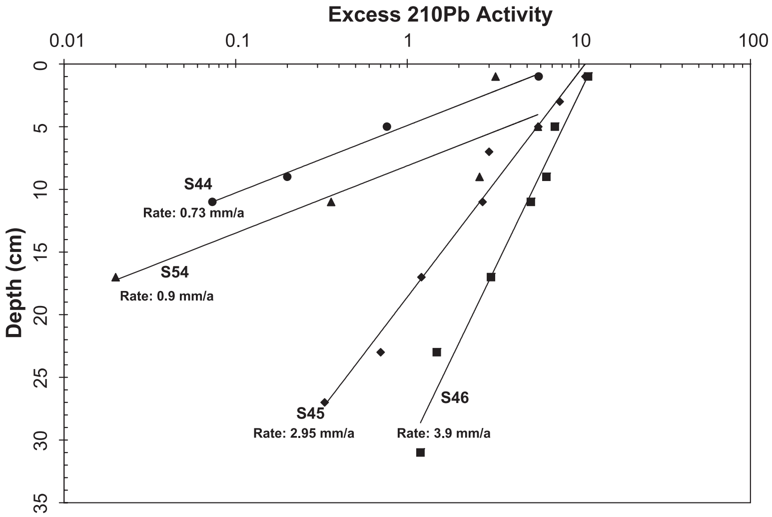

Fig. 16. Activity profile for unsupported (excess) ^{210}Pb of S44, S45, S46, S54, and their linear regression plots with their estimated sedimentation rates. Core locations are shown in Fig. 3.

exposed during the last glacial maximum (LGM) lowstand of sea level. Together with climate, which has influenced sediment input, the rise of post-LGM sea level has played a critical role in the development of the Shandong clinoform. Using an extensive sea-level database, Liu (2001) have demonstrated that the post-LGM transgression in the EC/YS and South China Sea was step-like: long periods of slow transgression (2–8 mm/year) punctuated by several short, rapid flooding events (~ 80 mm/year) (Fig. 18). By about 15 ka (calendar years), rising sea level had reached about 100 m (relative to present-day sea level), and seawater had begun to enter the central SYS. A rapid rise during melt water pulse 1A (MWP-1A,

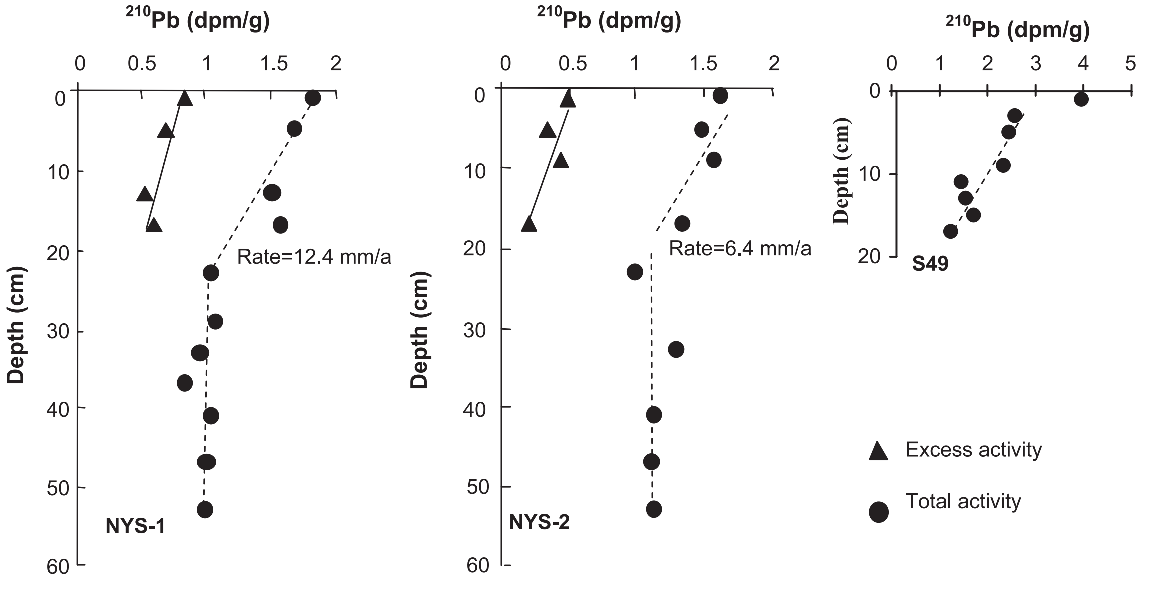

Fig. 17. Activity profile for total and excess ^{210}Pb of the core NYS-1, NYS-2, and S49 on the topset. Core locations are shown in Fig. 3.

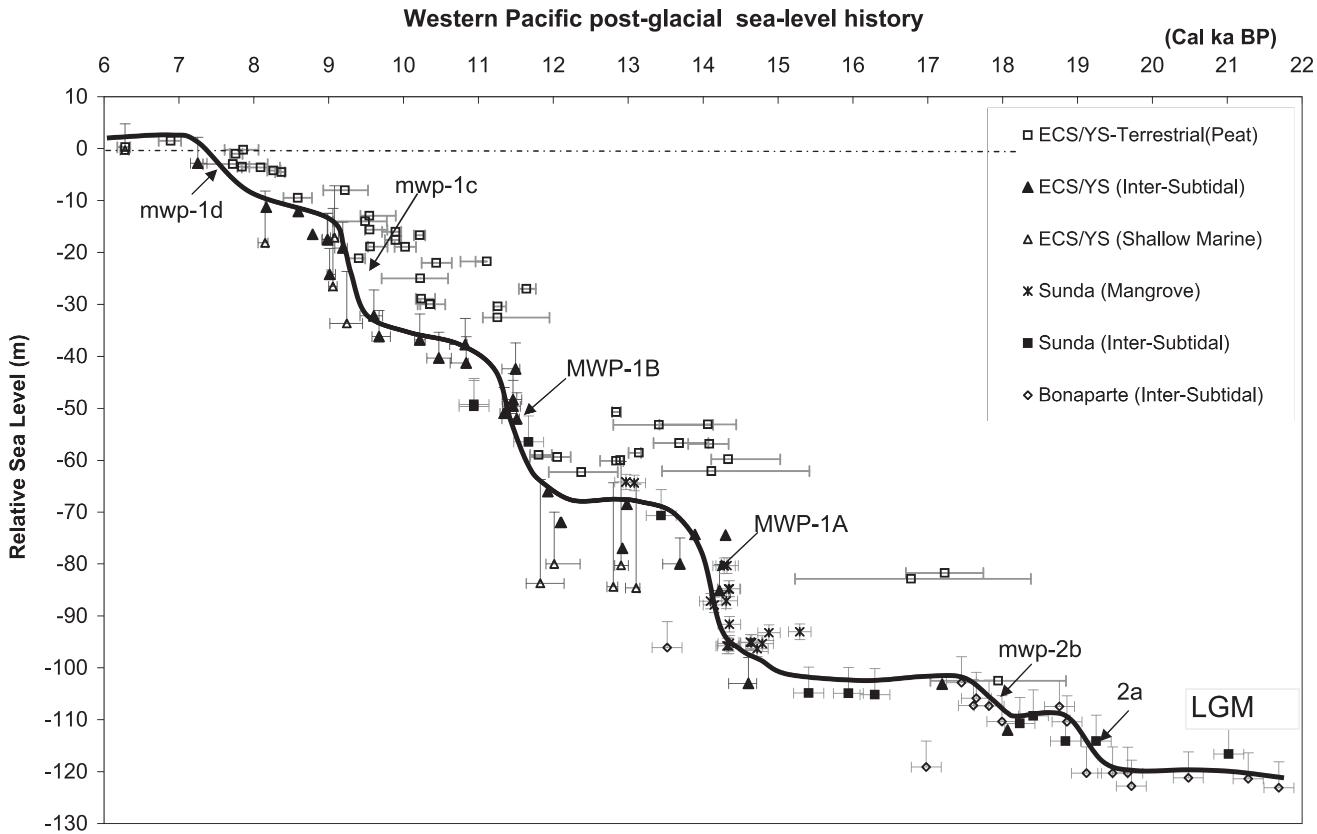

Fig. 18. Stepwise postglacial sea-level rise in the western Pacific (YS, ECS, and SCS). The episodic sea-level curve is defined based on extensive collections of sea-level indicators (fresh water peat, brackish and shallow marine) from the nearshore and submerged continental shelves of ECS (Liu, 2001), Sunda (Hanebuth et al., 2000), and Bonaparte Sea (Yokoyama et al., 2000).

Fairbanks, 1989; Bard et al., 1990; Hanebuth et al., 2000) occurred between 14.3 and 14.1 ka, when sea level jumped from 95 to 80 m (80 mm/year) transgressing horizontally several to many hundred meters per year. At the end of this MWP-1A flooding event, sea level had reached the southern edge of the NYS. For the ensuing 2500 years, sea level rose slowly (8 mm/year) from 80 to 60 m. Beginning ~ 11.6 ka, sea level again jumped from 58 to 43 m (MWP-1B of Fairbanks), resulting in a rapid westward flooding of the NYS and initial entrance into the Bohai Sea. Sea-level rise again stagnated (between − 42 to − 38 m) for about 1.8 ky, during which much of the early phase of Shandong clinoform accumulated.

To supply enough sediment into the Shandong clinoform, however, we need a sediment source as well as a slow down in the rate of sea-level transgression. Recent paleoclimatic data suggest that before the intensification of thde SW monsoon (about 11 ka; Wang et al., 1999), the Yellow River watershed may have been dry (Zhao, 1991). The presence of thick loess deposits along the northern Shandong Peninsula (Liu and Zhao, 1995) and evidence of relict loess in the shallow sub-bottom NYS sediments (see above) lend evidence of an arid glacial climate and therefore a dry Yellow River. Well-preserved peaty sediments and possible relict loess deposits indicate little fluvial input, and we find no evidence on our seismic profiles of buried or infilled river channels in this area. We thus conclude that before the intensification of the summer monsoon about 11 ka, the Yellow River was at best a minor sediment source.

Evidence of a dramatic intensification of the southwestern (summer monsoon) about 11 ka has been noted throughout southern Asia (Wang et al., 1999), and the initiation of maximum runoff and sediment discharges also has been observed in other climate-controlled Asian river systems, such as the Indus (Prins and Postma, 2000) and Ganges–Brahmaputra (Goodbred and Kuehl, 2000). We suggest that it was during this period 1.8-ky interval (11–9.2 ka BP: between MWP-1B and 1C) of slow-rising sea level and increased Yellow River discharge that the proximal Yellow River subaqueous delta accreted over the relict or transgressive facies along the northern shore of Shandong Peninsula (Fig. 19A). The acoustically turbid nature of the lower portion of the clinoform suggests that organic material was stored in this rapidly accreting proximal clinoform (Figs. 8–10).

Existence of pre-Holocene peat (~ 11 k cal BP) beneath the mud wedge is another strong evidence for the increasing monsoonal rainfall on the shelf. After the river delivered its first phase proximal sediment over the transgressive layer, the decomposed underlying organic-rich peaty sediment continued to provide the source of the gas to the overlying sediment (silt to silty mud). The acoustically transparent upmost layer (fine mud deposits) appears to be relatively gas-free. This phenomenon also can be seen other global deltaic systems, such as the Amazon (Nittrouer et al., 1996), Ebro (Diaz et al., 1996), and Po (Cattaneo et al., 2003), etc.

Beginning ~ 9.8 ka, sea level again rose rapidly, from 36 to 16 m in ~ 800 years (~ 45 mm/year), a flooding event that we have termed MWP-1C (Fig. 18). During this period of rapid transgression, extreme flooding of the Yellow River at 9.2 ka (Yang et al., 2000) appears to have diverted the river to the Jiangsu coast south of the Shandong Peninsula. This would explain the existence of the flooding surface (FS) in the seismic profiles (Figs. 9 and 10) as well as the prominent deltaic sequence noted off the Jiangsu coast (Milliman et al., 1989). The combination of the diverted flow and rapid sea-level rise resulted in little or no Yellow River sediment input to the Shandong clinoform. After ~ 7 ka BP, the river apparently diverted back to the north, but by this time another pulse of rapidly transgressing sea level (what we term MWP-1D) had pushed the shoreline 200 km westward. It was during this distal phase of the Yellow River that the acoustically transparent facies of the clinoform began to accumulate (Fig. 19B), a supposition that is borne out by the following calculations.

By dividing the NYS subaqueous clinoform into a proximal phase between 11 and 9.2 ka (Fig. 19A) and a distal phase after 9.2 ka (Fig. 19B), we can calculate a rough sediment budget. Based on the thickness of the mud distribution (Fig. 19), using the digital tools in ArcView-GIS, total sediment volume of the proximal phase is about 150 km^3 or (assuming a specific gravity of 1.2 t/m^3) 180×10^9 t. Assuming accumulation over 1.8 ky, when the sea level stood at about − 40 m, and the old Yellow river emptied directly into the NYS (Fig. 19A), this yields a mean sediment deposition of 0.1×10^9 t/year. While the proximal phase sediment

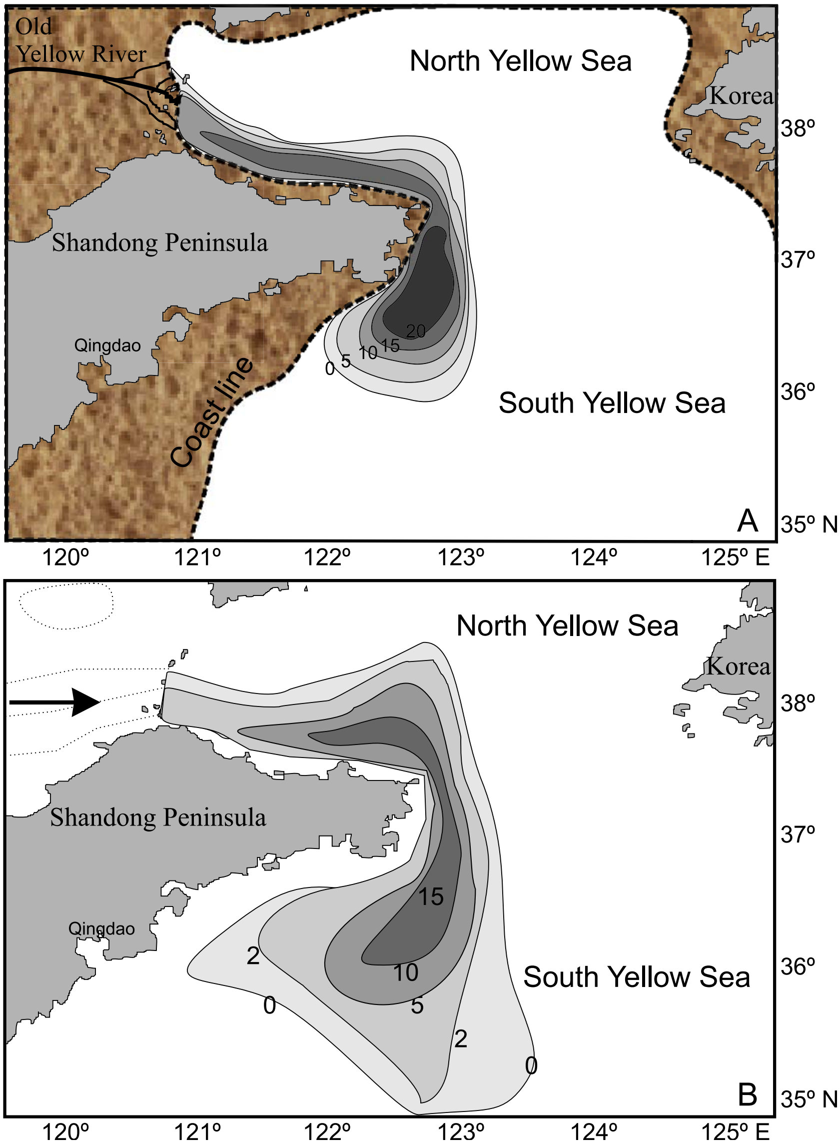

Fig. 19. Proximal (A) and distal (B) mud isopach around the Shandong Peninisula. The dash line in top (A) represents the paleo-coast line (~ −40 m) formed around 11 ka BP after MWP-1B sea-level rise. The Yellow River is believed to flow into the NYS at that time.

accumulation rate from the Yellow River in the NYS is about an order of magnitude lower than the modern river load in the Bohai (0.9×10^9 t/year; Galler, 1999), it appears to correspond closely with estimated pre-agriculture loads (e.g., Milliman et al., 1987; Saito et al., 2001). The overlying distal phase (Fig. 19) resulted in accumulation of an estimated 250 km^3 or 300×10^9 t of sediment in about 9000 years, giving an accumulation rate of 0.033×10^9 t/year (or 33×10^6 t/year), 1/3 that during the proximal phase. Given the 200-km distance between the modern river mouth and the clinoform, as well as the fact that for more than 800 years the river discharged south onto the Jiangsu coast, one might express surprise that the distal rate of sediment was not lower. This average sediment accumulation of 33×10^6 t/year is much higher than the 6–

8×10^6 t/year that Qin and Li (1986) and Martin et al. (1993) estimated presently escapes from the Bohai, suggesting that there may be other sources of sediment to the distal clinoform. This supposition is supported by mineralogical data that show that surficial sediments from the topset and foreset strata differ rather strongly from modern Yellow River sediments (Liu et al., 1987; Qin et al., 1989), suggesting that the small local streams and coastal erosion along the northern coast of the Shandong Peninsula may have contributed sediment to the clinoform (Fig. 20). We also note that the bottom part of the foreset slope (which we have called the "toe") has prograded not only northward (Figs. 10 and 11), but also to the east (Figs. 8 and 9), in agreement with the grain size distribution (Cheng and Gao, 2000; Figs. 14 and 15) and regional circulation patterns (Figs. 5, 6, and 20). The finer sediments in the central basin (Fig. 14) suggest net deposition, which is also shown by the greater sediment thickness in profile 98a (Fig. 12).

Seaward growth of the clinoform occurs primarily by overlap of along-shore and across-shore mud transport, creating a superimposed clinoform deposit. Along-shore and seaward surface flow in the upper layer also transport suspended sediment along and across shelf Figs. 14, 19, and 20). The upwelling and counter current in the deep layer of the boundary areas in the east Shandong Peninsula and NYS could allow landward supply of predeposited fine sediment to mud wedge. The strong YSWC and tide currents also may play an important role of eroding fine sediments in the northeastern NYS and transporting them southwestward to the Shandong mud wedge. This basin-wide cyclonic gyre system is considered to play an important role in trapping the fine sediments in the central NYS and SYS basins (Hu, 1984, Shen et al., 1996). Collectively, these geological and hydrological processes, together with input of Yellow River-derived sediment from Bohai, have helped form the morphology and shallow stratigraphy of the Shandong mud wedge and clinoform (Fig. 20).

6. Discussions and conclusions

Most subaqueous clinoforms' development and resultant geometry are mainly controlled by the interplay of sediment supply, depositional environment, and history of relative sea level. Formation of the Shandong clinoform reflects an interesting combination of the stepwise postglacial sea-level rise, reintensification of the Asian summer monsoon, and the shifting of the river mouth between the Bohai Sea and the southern Yellow Sea. As a result, and in contrast to other clinoforms, the Shandong clinoform appears to be a compound subaqueous deltaic system with what we interpret to be proximal and distal phases of clinoform development.

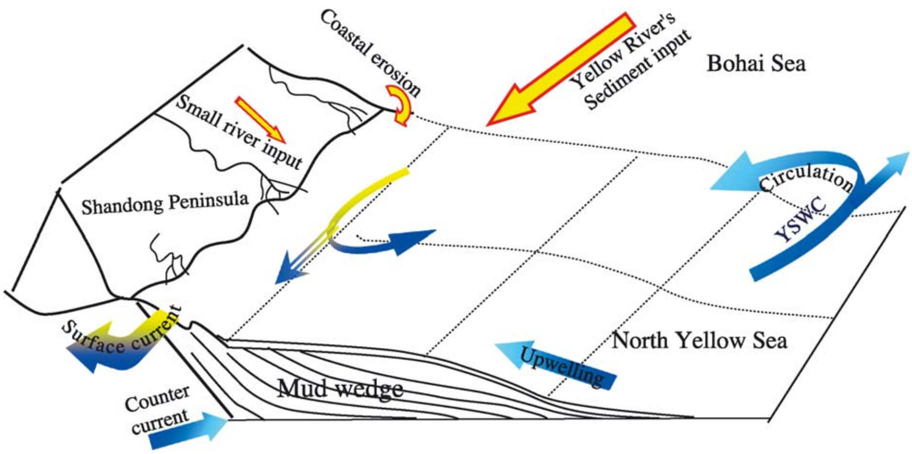

Fig. 20. Sedimentary processes affecting the morphology of the Yellow River subaqueous delta in the North Yellow Sea—the progradation of the clinoform mud wedge wraps around north and south of the Shandong Peninsula.

Because of the asymmetry of the late Quaternary glacio-eustatic cycles, most preserved sedimentary records on the modern outer shelves (>100 m) correspond to forced regressive deposits and thick lowstand system tract (LST), for instance, the outer shelf of the East China Sea (Berne et al., 2002, Saito et al., 1998) and the Sunda Shelf (Hanebuth et al., 2003). With the subsequent rapid sea-level rise and landward coastline migration, transgressive system tract (TST) began to develop extensively on the shelves, which can be recognized through a gradual or irregular landward shift of transgressive facies culminating with a maximum flooding surface (mfs) (Cattaneo and Steel, 2003). On a broad, flat epicontinental shelf lacking ample fluvial input pre-Holocene, the sea-level rise during MWP-1A or 1B could have advanced landward very rapidly without the stacking of any thick TST (Fig. 21). Instead, relict sand, thin transgressive sand deposits, and tidal-induced sand ridges can be formed and extensively distribute in the middle shelves (Emery, 1968; Liu et al., 2000; Berne et al., 2002). The TST underlying the Shandong clinoform presents the sediment stacking formed during the MWP-1B rapid sea-level rise between 11.6 and 11.2 ka BP (Figs. 18 and 21).

After the rapid rise of sea level (MWP-1B) and reinitiation of the summer monsoon at 11 ka BP, a large amount of river-derived sediment was delivered to the ocean and deposited over the previous (TST). As discussed earlier, the Yellow River-derived deposits began to accumulate in the NYS after MWP-1B, ~ 11 ka BP, about the same time the Yangtze, G–B, Indus, Mekong, and other Asian rivers experienced increased discharge and sediment loads: (Chen et al., 2000; Goodbred and Kuehl, 2000; Prins and Postma, 2000; Ta et al., 2002). The timing of European clinoforms and deltas follow a somewhat similar chronology, apparently in response to both changes in sea-level rise and sediment delivery. The Ebro River's distal prodelta mud deposits, for example, overlie a relict transgressive sand at 60–80-m water depth, with ^{14}C ages between 10,000–11,000 years (Diaz et al., 1996). After Younger Dryas (12.8–11.6 ka) cold event and decelerated sea-level rise (11 ka), the Guadinna River

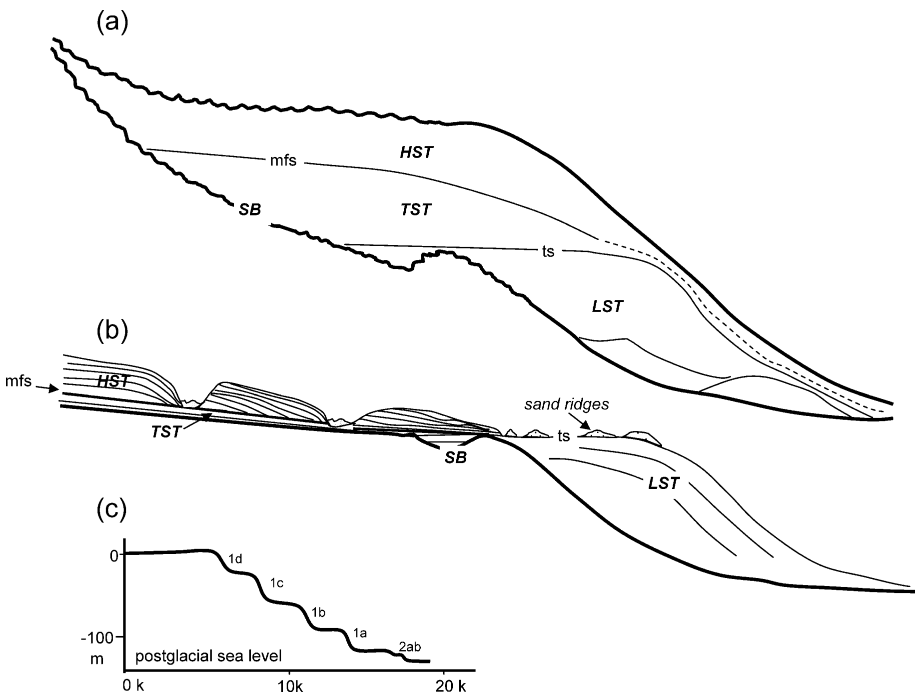

Fig. 21. Simplified diagram (after Trincardi et al., 1994) shows different sequence stratigraphy models between pericontinental (a) and epicontinental (b) (e.g., ECS and YS) margins under a high-amplitude stepwise postglacial sea-level rise (c) (Liu, 2001).

began to deliver sediment to the mid-shelf of Gulf of Cadiz (Lobo et al., 2001).

Rapid sea-level rise during MWP-1B provided new accommodation space that could be quickly filled during the subsequent lull in sea-level rise, and it was during this period that the proximal portion of the Shandong clinoform was formed. The geometry of this portion of the clinoform was sigmoidal, as is common in clinoforms that form proximal to river mouths (Christie-Blick and Driscoll, 1995). After MWP-1C, ~ 9 ka BP, however, the Huanghe's mouth shifted southward into the south Yellow Sea. By the time the river again shifted northward, ~ 7 ka BP, sea level had risen to + 2–3 m, and the Huanghe's mouth was now several hundred kilometers from the Shandong clinoform. The distal portion of the clinoform appears to have become monoclinal, similar to the way Driscoll and Karner's (1999) three-dimensional numerical model would predict a clinoform to form away from the source (Driscoll and Karner, 1999). A similar pattern is seen in a number of clinoforms, such as the Amazon (Nittrouer et al., 1996), Ebro (Diaz et al., 1996), and Po (Trincardi et al., 1994, Cattaneo et al., 2003). Driscoll and Karner's 3-D model also shows an onlap surface that can be generated when the sediment is transported along shelf away from the sediment source. For the most part, the Shandong clinoform does not follow this rule; instead, it has downlap deposits prograding over a relict transgressive layer in the toe region (see profiles 99-A, 99-B, and 99-F; Figs. 8–10). In a similar way, seismic profiles from the center of the Canterbury Basin, New Zealand, demonstrate that downlap surfaces of highstand system tract (HST) overlie previously deposited toe-of-clinoform sediment (Carter et al., 1998).

More interestingly, different from other river systems, the Yellow River deltaic deposits indicate a very unique way dispersing its sediment to the ocean, where they are influenced uniquely by formation of the negatively (hyperpycnal) buoyant sediment plumes, seasonal resuspension, and longshore current transportation. The dominant negatively hyperpycnal plumes travel very shorter distance near the modern Yellow River mouth (Wright et al., 2001); after that, the Yellow River-derived fine sediments are resuspended, mainly in winter seasons, and are continually transported long distance along margins in a semihyperpycnal flow (Fig. 6). Together with the along-shelf transport, cross-shelf advection appears to play an important role in the development of a clinoform downstream from the sediment source-river mouth. We suggest that when a precipitous change of the coastal configuration occurs, along-shore sediment transport can shift to cross-shore transport. For instance, around the eastern end of the Shandong Peninsula, alongshore sediment transport appears to change from east to south. A similar situation is seen in the Adriatic Sea, where the Gargano promontory shifts along-shore transport and increases cross-shore transport (Cattaneo et al., 2003). The change from along-shore to cross-shore transport may explain the sequence stratigraphic shift from aggradational onlap to progradational downlap.

Acknowledgements

Many thanks to the crews of RV *Goldstar II* and our Chinese and American colleagues for their help in obtaining and processing data. We thank L.D. Wright, Y. Saito, S. Kuehl N. Driscoll, and Z.S. Yang for their many helpful comments on an earlier version of this paper. Financial supports for this program from National Science Foundation of U.S. and China, the Office of Naval Research. And many thanks Woods Hole Oceanographic Institution's Postdoctoral Scholar Program with funding provided by the U.S. Geological Survey to Liu. This is also contribution no. 2612 from Virginia Institute of Marine Science, College of William & Mary.

References

Alexander, C.R., DeMaster, D.J., Nittrouer, C.A., 1991. Sediment accumulation in a modern epicontinental-shelf setting: the Yellow Sea. Marine Geology 98, 51–72.

Bard, E., Hamelin, B., Fairbanks, R.G., 1990. U–Th ages obtained by mass spectrometry in corals from Barbados: sea level during the past 130 000 years. Nature 346 (6283), 456–458.

Berne, S., et al., 2002. Pleistocene forced regressions and tidal sand ridges in the East China Sea. Marine Geology 188 (3–4), 293–315.

Bornhold, B.D., Yang, Z.S., Keller, G.H., Prior, D.B., Wiseman, W.J., Wang, Q., Wright, L.D., Xu, W.D., Zhuang, Z.Y., 1986. Sedimentary framework of the modern Huanghe (Yellow River) Delta. Geo-Marine Letters 6, 77–83.

Carter, R.M., Fulthorpe, C.S., Naish, T.R., 1998. Sequence concepts at seismic and outcrop scale: the distinction between physical and conceptual stratigraphic surfaces. Sedimentary Geology 122 (1–4), 165–179.

Cattaneo, A., Steel, R.J., 2003. Transgressive deposits: a review of their variability. Earth-Science Reviews 62 (3–4), 187–228.

Cattaneo, A., Correggiari, A., Langone, L., Trincardi, F., 2003. The late-Holocene Gargano subaqueous delta, Adriatic shelf: sediment pathways and supply fluctuations. Marine Geology 193 (1–2), 61–91.

Chen, Z.Y., Song, B.P, Wang, Z.H, Cai, Y.L, 2000. Late Quaternary evolution of the sub-aqueous Yangtze Delta, China: sedimentation, stratigraphy, palynology, and deformation. Marine Geology 162, 243–441.

Cheng, P., Gao, S., 2000. Net sediment transport patterns over the northwestern Yellow Sea, based on grain-size tread analysis. Oceanologia et Limnologia Sinica 31 (6), 604–615.

Christie-Blick, N., Driscoll, N.W., 1995. Sequence stratigraphy. Annual Review of Earth and Planetary Sciences 23, 451–478.

Cutshall, N.H., Larsen, I.L., Olsen, C.R., 1983. Direct analysis of ^{210}Pb in sediment samples: shelf-absorption correction. Nuclear Instruments and Methods 206, 309–312.

Diaz, J.I., Palanques, A., Nelson, C.H., Guillen, J., 1996. Morphostructure and sedimentary of the Holocene Ebro prodelta mud belt (northwestern Mediterranean Sea). Continental Shelf Research 16 (4), 435–456.

Driscoll, N.W., Karner, G.D., 1999. Three-dimensional quantitative modeling of clinoform development. Marine Geology 154 (1–4), 383–398.

Emery, K.O., 1968. Relict sediments on continental shelves of world. American Association of Petroleum Geologists Bulletin 52 (3), 445–464.

Fairbanks, R.G., 1989. A 17,000-year glacio-eustatic sea level record: influence of glacial melting rates on the Younger Dryas event and deep ocean circulation. Nature 342, 637–642.

Galler, J.J., 1999. Medium and long-term changes in fluvial discharge to the sea: the Yellow River case study. Master of Science thesis, College of William & Mary, 78 pp.

Goodbred, S.L., Kuehl, S.A., 2000. The significance of large sediment supply, active tectonism, and eustasy on margin sequence development: Late Quaternary stratigraphy and evolution of the Ganges–Brahmaputra delta. Sedimentary Geology 133, 227–248.

Guan, B.X., 2000. Inversion thermocline in coastal region north and east of Shandong Peninsula in winter and its relation to deep-bottom counter current. Journal of Oceanography of Huanghai & Bohai Seas 18 (3), 66–71.

Hanebuth, T., Stattegger, K., Grootes, P.M., 2000. Rapid flooding of the Sunda Shelf: a late-glacial sea-level record. Science 288, 1033–1035.

Hanebuth, T.J.J., Stattegger, K., Schimanski, A., Ludmann, T., Wong, H.K., 2003. Late Pleistocene forced-regressive deposits on the Sunda Shelf (Southeast Asia). Marine Geology 199 (1–2), 139–157.

Hu, D.X., 1984. Upwelling and sedimentation dynamics. Chinese Journal of Oceanology and Limnology 2 (1), 12–19.

Jiang, W.S., Pohlmann, T., Sundermann, J., Feng, S.Z, 2000. A modeling study of SPM transport in the Bohai Sea. Journal of Marine Systems 24, 175–200.

Kim, Y.H., Chough, S.K., Lee, H.J., Chun, S.S., Han, S.J., 1999. Holocene transgressive stratigraphy of a macrotidal flat in the southeastern Yellow Sea: Gomso Bay, Korea. Journal of Sedimentary Research. Section B, Stratigraphy and Global Studies 69 (2), 328–337.

Kuehl, S.A., DeMaster, D.J., Nittrouer, C.A., 1986. Nature of sediment accumulation on the Amazon continetal shelf. Continental Shelf Research 6, 209–225.

Kuehl, S.A., Levy, B.M., Moore, W.S., Allison, M.A, 1997. Subaqueous delta of the Ganges–Brahmaputra river system. Marine Geology 144, 81–96.

Li, F., Ding, Z.X., 1996. Vertical distribution patterns of suspended matter and near bottom turbid water layer in the South Yellow Sea. Studia Marina Sinica 37, 33–42.

Liu, J.P., 2001. Post-glacial sedimentation in a river-dominated epicontinental shelf: the Yellow Sea example. PhD Dissertation, College of William & Mary, VA, USA.

Liu, J.P., Zhao, S.L., 1995. Origin of the buried loess in the Bohai Sea bottom and the exposed loess along the coastal zone. Oceanologia et Limnologia Sinica 26, 363–368.

Liu, M.H., Wu, S.Y., Wang, Y.J., 1987. Late Quaternary Sediments of the Yellow Sea. China Ocean Press, Beijing, p. 433.

Liu, Z.X., Xia, D.X., Berne, S., Wang, K.Y., Marsset, T., Tang, Y.X., Bourillet, J.F., 1998. Todal deposition systems of China's continental shelf, with special reference to the eastern Bohai Sea. Marine Geology 145, 225–253.

Liu, Z.-X., Berne, S., Saito, Y., Lericolais, G., Marsset, T., 2000. Quaternary seismic stratigraphy and paleoenvironments on the continental shelf of the East China Sea. Journal of Asian Earth Sciences 18 (4), 441–452.

Liu, J.P., Milliman, J.D., Gao, S., 2002. The Shandong mud wedge and post-glacial sediment accumulation in the Yellow Sea. Geo-Marine Letters 21, 212–218.

Lobo, F.J., Hernandez-Molina, F.J., Somoza, L., Diaz del Rio, V., 2001. The sedimentary record of the post-glacial transgression on the Gulf of Cadiz continental shelf (Southwest Spain). Marine Geology 178 (1–4), 171–195.

Martin, J.M., Zhang, J., Shi, M.C., Zhou, Q., 1993. Actual flux of the Huanghe (Yellow River) sediment to the western Pacific Ocean. Netherlands Journal of Sea Research 31, 243–254.

McManus, J., 1988. Grain-size determination and interpretation. In: Tucker, M. (Ed.), Techniques in Sedimentology. Blackwell, Oxford, pp. 63–85.

Milliman, J.D., Meade, R.H., 1983. World-wide delivery of river sediment to the oceans. Journal of Geology 91, 1–21.

Milliman, J.D., Syvitski, J.P.M., 1992. Geomorphic/tectonic control of sediment discharge to the ocean: the importance of small mountainous rivers. Journal of Geology 100, 525–544.

Milliman, J.D., Li, F., Zhao, Y.Y., Zheng, T.M., Limeburner, R., 1986. Suspended matter regime in the Yellow Sea. Progress in Oceanogography 17, 215–227.

Milliman, J.D., Qin, Y.S., Ren, M.E., Saito, Y., 1987. Man's influence on the erosion and transport of sediment by Asian rivers: the Yellow River (Huanghe) example. Journal of Geology 95, 751–762.

Milliman, J.D., Qin, Y.S., Park, Y., 1989. Sediment and sedimentary processes in the Yellow and East China Seas. In: Taira, A., Masuda, F. (Eds.), Sedimentary Facies in the Active Plate Margin, Terra Scientific, Tokyo, pp. 233–249.

Morgan, J.P., 1970. Deltaic Sedimentation: Modern and Ancient. SEPM Special Publication 15, 312 pp.

Nittrouer, C.A., Kuehl, S.A., DeMaster, D.J., Kowsmann, R.O., 1986. The deltaic nature of Amazon shelf sedimentation. Geological Society of America Bulletin 97, 444–458.

Nittrouer, C.A., Kuehl, S.A., Figueiredo, A.G., Allison, M.A., Sommerfield, C.K., Rine, J.M., Faria, L.E.C., Silveira, O.M., 1996. The geological record preserved by Amazon shelf sedimentation. Continental Shelf Research 16, 817–841.

Park, Y.A., Lim, D.I., Khim, B.K., Choi, J.Y., Doh, S.J., 1998. Stratigraphy and subaerial exposure of Late Quaternary tidal deposits in Haenam Bay, Korea (south-eastern Yellow Sea). Estuarine, Coastal and Shelf Science 47 (4), 523–533.

Prins, M.A., Postma, G., 2000. Effects of climate, sea level, and tectonics unraveled for last deglaciation turbidite records of the Arabian Sea. Geology 28, 375–378.

Qian, N., Dai, D.Z., 1980. The problems of river sedimentation and present status of its research in China. Chinese Hydraulic Engineering, Proceedings of the International Symposium of River Sedimentation 1, 1–39.

Qin, Y.S., Li, F., 1986. Study of the influence of sediment loads discharged from Huanghe river on sedimentation in the Bohai and Yellow Seas. Oceanologia et Limnologia Sinica 27, 125–135.

Qin, Y.S., Zhao, Y.Y., Chen, L.R., Zhao, S.L., 1989. Geology of the Yellow Sea. China Ocean Press, Beijing, p. 289.

Saito, Y., Yang, Z.S., 1995. Historical change of the Huanghe (Yellow River) and its impact on the sediment budget of the East China Sea. In: Tsunogai, S., Iseki, K., Koike, I., Oba, T. (Eds.), Global Fluxes of Carbon and Its Related Substances in the Coastal Sea–Ocean–Atmosphere System. M&J International, Yokohama, pp. 7–12.

Saito, Y., Katayama, H., Ikehara, K., Kato, Y., Matsumoto, E., Oguri, K., Oda, M., Yumoto, M., 1998. Transgressive and highstand systems tracts and post-glacial transgression, the East China Sea. Sedimentary Geology 122, 217–232.

Saito, Y., Yang, Z.S., Hori, K., 2001. The Huanghe (Yellow River) and Changjiang (Yangtze River) deltas: a review on their characteristics, evolution and sediment discharge during the Holocene. Geomorphology 41, 219–231.

Shen, S.X., Li, A.C., Yuan, W., 1996. Low energy environment of the central South Yellow Sea. Oceanologia et Limnologia Sinica 27 (5), 518–523.

Stuiver, M., Reimer, P.J., Bard, E., Beck, J.W., Burr, G.S., Hughen, K.A., Kromer, B., McCormac, F.G., v. d. Plicht, J., Spurk, M., 1998. INTCAL98 radiocarbon age calibration 24,000-0 cal BP. Radiocarbon 40, 1041–1083.

Sun, X.G., Fang, M., Huang, W., 2000. Spatial and temporal variations in suspended particulate matter transport on the Yellow and East China Sea shelf. Oceanologia et Limnologia Sinica 31 (6), 581–587.

Ta, T.K.O., Nguyen, V.L., Tateishi, M., Kobayashi, I., Tanabe, S., Saito, Y., 2002. Holocene delta evolution and sediment discharge of the Mekong River, southern Vietnam. Quaternary Science Reviews 21, 1807–1819.

Trincardi, F., Correggiari, A., Roveri, M., 1994. Late Quaternary transgressive erosion and deposition in a modern epicontinental shelf: the Ariatic Semienclosed Basin. Geo-Marine Letters 14, 41–51.

Wang, L., Sarnthein, M., Erlenkeuser, H., Grimalt, J., Grootes, P., Heilig, S., Ivanova, E., Kienast, M., Pelejero, C., Pflaumann, U., 1999. East Asian monsson climate during the Late Pleistocene: high-resolution sediment records from the South China Sea. Marine Geology 156, 245–248.

Wright, L.D., Coleman, J.M., 1973. Variation in morphology of major deltas as functions of ocean wave and river discharge regime. AAPG Bulletin 57, 370–398.

Wright, L.D., Wiseman, W.J., Bornhold, B.D., Prior, D.B., Suhayda, J.N., Keller, G.H., Yang, Z.S., Fan, Y.B., 1988. Marine disperal and deposition of Yellow River silts by gravity-driven underflows. Nature 332, 629–632.

Wright, L.D., Wiseman, W.J., Yang, Z.S., Bornhold, B.D., Keller, G.H., Prior, D.B., Suhayda, J.N., 1990. Processes of marine dispersal and deposition of suspended silts off the modern mouth of the Huanghe (Yellow River). Continental Shelf Research 10, 1–40.

Wright, L.D., Friedrichs, C.T., Kim, S.C., Scully, M.E., 2001. Effects of ambient currents and waves on gravity-driven sediment transport on continental shelves. Marine Geology 175 (1–4), 25–45.

Xia, Z.W., Guo, B.H., 1983. Cold water and upwelling around the tips of Shandong Peninsula and Liaodong Peninsula. Journal of Oceanography of Huanghai & Bohai Seas 1, 13–19.

Yanagi, T., Inoue, K., 1995. A numerical experiment on the sedimentation processes in the Yellow Sea and the East China Sea. Journal of Oceanography 51, 537–552.

Yang, Z.S., Milliman, J.D., Galler, J., Liu, J.P., Sun, X.G., 1998. Yellow river's water and sediment discharge decreasing steadily. EOS 79 (48), 589–592.

Yang, D.Y., Yu, G., Xie, Y.B., Zhan, D.J., Li, Z.J., 2000. Sedimentary records of large Holocene floods from the middle reaches of the Yellow River, China. Geomorphology 33, 73–88.

Yokoyama, Y., Fifield, L.K., Lambeck, K., De Deckker, P., Johnston, P., 2000. Timing of the Last Glacial Maximum from observed sea-level minima. Nature 406 (6797), 713–716.

Yuan, Y., Su, J., 1984. Numerical modelling of the circulation in the East China Sea. In: Ichiiye, T. (Ed.), Ocean Hydrodynamics of Japan and East China Sea. Elsevier Oceanography Series, vol. 39. Elsevier, New York, pp. 167–186.

Zhao, S.L., 1991. China shelf sea desertization and its derived deposits during the last stage of Late Pleistocene. Oceanologia et Limnologia Sinica 22 (3), 285–293.

Zhao, B.R., 1996. A study of the circulations of the northern Yellow Sea cold water mass—effects of tidal mixing on them. Oceanologia et Limnologia Sinica 27 (4), 429–435.

Zheng, Q.A., Klemas, V., 1982. Determination of winter temperature patterns, fronts, and surface currents in the Yellow Sea and East China Sea from satellite imagery. Remote Sensing of Environment 12, 201–218.